Identification of a common immune regulatory pathway induced by small heat shock proteins, amyloid fibrils, and nicotine

Jonathan B. Rothbard[a], Jesse J. Rothbard[b], Luis Soares[b], C. Garrison Fathman[b], and Lawrence Steinman[a,1]

[a]Department of Neurology, Stanford University School of Medicine, Stanford, CA 94305-5316; and [b]Department of Medicine, Stanford University School of Medicine, Stanford, CA 94305-5316

Contributed by Lawrence Steinman, May 28, 2018 (sent for review March 20, 2018; reviewed by Lars Fugger and Kevin J. Tracey)

Although certain dogma portrays amyloid fibrils as drivers of neurodegenerative disease and neuroinflammation, we have found, paradoxically, that amyloid fibrils and small heat shock proteins (sHsps) are therapeutic in experimental autoimmune encephalomyelitis (EAE). They reduce clinical paralysis and induce immunosuppressive pathways, diminishing inflammation. A key question was the identification of the target for these molecules. When sHsps and amyloid fibrils were chemically cross-linked to immune cells, a limited number of proteins were precipitated, including the α7 nicotinic acetylcholine receptor (α7 NAChR). The α7 NAChR is noteworthy among the over 20 known receptors for amyloid fibrils, because it plays a central role in a well-defined immune-suppressive pathway. Competitive binding between amyloid fibrils and α-bungarotoxin to peritoneal macrophages (MΦs) confirmed the involvement of α7 NAChR. The mechanism of immune suppression was explored, and, similar to nicotine, amyloid fibrils inhibited LPS induction of a common set of inflammatory cytokines while inducing Stat3 signaling and autophagy. Consistent with this, previous studies have established that nicotine, sHsps, and amyloid fibrils all were effective therapeutics in EAE. Interestingly, B lymphocytes were needed for the therapeutic effect. These results suggest that agonists of α7 NAChR might have therapeutic benefit for a variety of inflammatory diseases.

α7 nicotinic acetylcholine receptor | amyloid fibrils | small heat shock proteins | EAE | immune suppression

Amyloid precursor protein and αB crystallin (HspB5) are found in copious quantities in multiple sclerosis lesions, including white matter and degenerating axons (1). A protective role for the small heat shock protein (sHsp) was established when HspB5-knockout mice were shown to exhibit greater paralytic symptoms of EAE than wild-type controls (2). Even though sHsps are intracellular, cytosolic proteins, daily i.v. or i.p. injection resulted in significant reduction of the clinical signs of EAE. Subsequent studies have demonstrated that HspB5 is effective in reducing the lesion size in a murine model of stroke (3), reducing inflammation and improving heart function in a model of myocardial infarction (4), and increasing oligodendroglial survival in the optic nerve in a model of retinal ischemia (5).

Structure-function studies of the sHsp revealed that residues 73 to 92 exhibited chaperone activity and that the peptide was equally therapeutic as the intact protein, reducing paralysis and histological neuroinflammation in EAE (6). The chaperone function and therapeutic activity depended on the peptide forming amyloid fibrils. Injection or inhalation of fibrils composed of amyloidogenic peptides as short as six amino acids from a variety of proteins induces several pathways of immune suppression, resulting in reduction of the proinflammatory cytokines IL-6, IL-1β, and TNF-α and reduction of T cell activation (7). The fibrils are bound specifically and endocytosed by peritoneal macrophages (MΦs) and B2 and B1a lymphocytes, but not T lymphocytes, mast cells, or eosinophils (8, 9). The binding results in changes in gene expression, leading to several coordinated antiinflammatory responses: (*i*) activation of the cells, defined as an increased expression of CD83, CD80, and CD86 on the MΦs, and of CD80, CD86, CD25, and CD83 on the B1a lymphocytes; (*ii*) decreased expression of integrins and chemokine receptors, which allows both cell populations to traffic from the peritoneum to secondary lymph organs; and (*iii*) evidence of continued high expression of IL-10 in both cell types, with induced expression of CTLA4, BTLA, IRF4, and Siglec G in the B1a cells, thus increasing their immune-suppressive potential. In the secondary lymph organs, both populations of IL-10–producing cells inhibit antigen presentation and T cell activation, thereby reducing consequent proinflammatory cytokine production, leading to reduction of the paralytic signs of EAE.

The proposed mode of action was supported by loss-of-function experiments using B cell-deficient (μMT) mice and IL-10–knockout animals (neither of which responded to the fibrils), which established the critical role of IL-10–secreting regulatory B cells (8). Reciprocal gain-of-function experiments, in which as few as 3×10^5 B1a cells were reintroduced into μMT mice, reconstituted the ability of the fibrils to ameliorate clinical paralysis. In addition to the recovery of the response, the experiment also demonstrated that the presence of the B1a cells without stimulation with the fibrils was insufficient for the therapeutic effect. Clinical paralysis was reduced only when the B1a cells were activated.

Mass spectral analyses of amyloid fibrils cross-linked to peritoneal cells revealed that the fibrils bound α7 nicotinic acetylcholine receptor (α7 NAChR), and *N*-methyl-D-aspartate (NMDA) receptor,

Significance

The identification of α7 nicotinic acetylcholine receptor (α7 NAChR) as the principal receptor for amyloid fibrils and small heat shock proteins clarifies their mechanism of immune suppression. The discovery of the receptor allows previous experiments using amyloid fibrils to be interpreted based on the extensive body of literature detailing the NAChR signaling pathway. In addition, the data further support the realization that amyloid fibrils are immune suppressive, which may be an important factor in neurodegenerative diseases. The demonstration that NAChR agonists are effective in limiting ischemia and autoimmunity emphasizes that the α7-specific partial agonists, which failed in clinical trials for Alzheimer's disease and schizophrenia, could be reconsidered as therapeutics for a spectrum of inflammatory indications.

Author contributions: L. Steinman designed research; J.B.R. and J.J.R. performed research; L. Soares contributed new reagents/analytic tools; J.J.R., C.G.F., and L. Steinman analyzed data; and J.B.R. and L. Steinman wrote the paper.

Reviewers: L.F., University of Oxford; and K.J.T., Donald and Barbara Zucker School of Medicine at Hofstra/Northwell.

Conflict of interest statement: L. Steinman and J.B.R. have a patent application filed via Stanford University on the work. The remaining authors declare no conflict of interest.

[1]To whom correspondence should be addressed. Email: steinman@stanford.edu.

This article contains supporting information online at www.pnas.org/lookup/suppl/doi:10.1073/pnas.1804599115/-/DCSupplemental.

Published online June 18, 2018.

subunit D, on peritoneal MΦs and B2 and B1a cells, but not T lymphocytes. Wang and colleagues previously reported that amyloid β bound α7 NAChR, signaling through Jak2 and Stat3 (10, 11). α7 NAChR is unique among the over 20 known receptors for amyloid fibrils, being central in a well-defined immune-suppressive pathway involving the vagus nerve (12). Nicotine induces a similar pattern of immune suppression comparable to what is observed with sHsps and amyloid fibrils and has been shown to be an effective therapeutic for EAE (13–17). In addition to binding α7 NAChR, nicotine, T7 HspB4, and amyloid fibrils composed of Tau 623-628 all (*i*) signal through Stat3, (*ii*) inhibit cell surface α-bungarotoxin binding, (*iii*) inhibit proinflammatory cytokine secretion, (*iv*) induce autophagy, and (*v*) are therapeutic in animal models of EAE. Nicotine, T7 HspB4, and amyloid fibrils all require both the expression of α7 NACHR and the presence of B1a lymphocytes to be effective. Collectively, the data support the conclusion that these compounds are NAChR agonists inducing a common pattern of immune suppression.

Results

Cross-Linking Amyloid Fibrils to Peritoneal MΦs and B and T Lymphocytes. Identification of the cell surface receptors for amyloid fibrils and sHsps required a strategy that covalently cross-linked the ligands to the receptors. The principal populations of peritoneal cells (MΦs and B1a, B2, and T lymphocytes) were purified by flow cytometry and grown in leucine- and methionine-deficient media in the presence of aziridine analogs of leucine and methionine. Each cell population was incubated with and without biotinylated Tau or biotinylated T7 HspB4, photolysed, and lysed, and the resultant biotinylated complexes were isolated using Neutravidin. Reduction and alkylation was followed by on-resin trypsinization. The resultant mixture of peptides was separated by HPLC and identified using mass spectrometry.

Elimination of background proteins seen in the paired samples that did not contain biotinylated Tau or T7 HspB4 resulted in only seven proteins seen in the MΦ and B2 and B1a lymphocyte samples treated with biotinylated T7 HspB4 (but not seen in T cells): the 2D subunit of NMDA glutamate receptor (Grin2D), α7 NAChR (Chrna7), KidIns220, UV radiation resistance associated protein (UVrag), dynein heavy chains 2 and 3, and Ras GTP-like activating protein (*SI Appendix*, Table S1). For samples treated with biotinylated Tau 623-628, six of the seven proteins were observed, with the GTP-binding protein RAN substituted for the RAS GTP-like activating protein (*SI Appendix*, Table S1). The results were consistent with the literature, which previously established that amyloid β binds NAChR (10, 11, 18–20) and associates with NMDA glutamate receptor (21). KidIns220 is a scaffolding protein with multiple ankyrin repeats binding the A and B subunits of NMDA in neuronal tissue (22) but is not documented to bind the D subunit of the NMDA receptor, which is principally expressed in nonneuronal tissue (23). There is extensive literature documenting α7 NAChR in all three cell types (12, 24–26), while UVrag is essential for autophagy and implicates the amyloid fibrils in this process.

α-Bungarotoxin Binding and Competition. Modulation of NMDA glutamate and NAChR signaling can ameliorate EAE, but in diametrically different ways. Therapeutic benefit is observed when the NAChR pathway is stimulated (13–16) or when NMDA signaling is inhibited (27). α7 NAChR, but not NMDA, signaling was investigated further because amyloid fibrils and sHsps appear to be agonists, stimulating pathways of immune suppression strikingly similar to those induced by nicotine (13–16). In addition, α7 NAChR is unique among amyloid receptors being integral to an endogenous immune-suppressive pathway involving the vagus nerve (12, 28).

When α-bungarotoxin was used to stain murine peritoneal cells isolated from wild-type C57BL/6, a closely related pattern to that generated by fluorescent analogs of Tau 623-628 and T7 HspB4 was observed (Fig. 1). The specificity of α-bungarotoxin mirrored

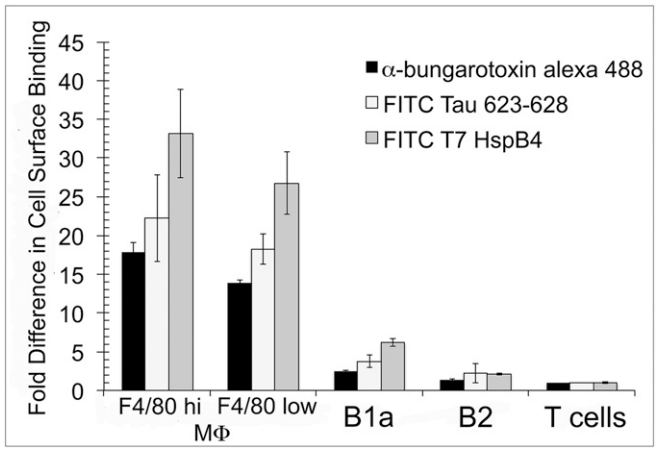

Fig. 1. α-Bungarotoxin, T7 HspB4, and amyloid fibrils composed of Tau 623-628 exhibit a similar pattern of cell surface binding to the predominant populations of murine peritoneal cells. Specific binding of fluorescent amyloid fibrils, T7 HspB4, and α-bungarotoxin were measured using flow cytometry. The data were normalized to the signal on T lymphocytes and plotted as differences in relative fold binding. Values in graph represent mean ± SD.

that of the fibrils and sHsp, binding both populations of MΦs at higher levels than B cells, which was two to three times greater than the signal of the T cells, consistent with the three molecules binding a common receptor.

A competitive whole-cell binding experiment was designed by preincubating HEK-293 fibroblasts, which express α7 NAChR (*SI Appendix*, Fig. S1), with varying concentrations of FITC-T7 HspB4 and with subsequent introduction of α-bungarotoxin labeled with Alexa 627. The mixture was incubated for 15 min at 4 °C and then the cells were washed, fixed, and analyzed using confocal microscopy (Fig. 2 *A–D*). Quantitation of the intensity of red and green light in eight micrographs, including the four shown in Fig. 2 *A–D*, demonstrate that increasing the T7 HspB4 concentration from 15 to 30 μM reduced Alexa 647 α-bungarotoxin binding by an average of 53% (*SI Appendix*, Table S2).

An additional competitive experiment demonstrated that increasing amounts of Tau 623-628 also could reduce the binding of α-bungarotoxin ∼60% when measured by mean fluorescence using flow cytometry (Fig. 2*E*) or replotted as percent inhibition (Fig. 2*F*). The ability of T7 HspB4 and Tau 623-628 to compete with α-bungarotoxin strengthens the hypothesis that the Tau 623-628 and T7 HspB4 are binding to α7 NAChR.

α7 NaChR Signaling. Previous studies established that activation of α7 NAChR results in Jak2 phosphorylation and subsequent phosphorylation of Stat3, which dimerizes, migrates to the nucleus, and binds SIE sequence in Stat3-inducible genes (29, 30). To determine whether amyloid fibrils and sHsps also stimulate this pathway, HEK-293 cells were transfected with a commercially available reporter plasmid with the SIE promoter juxtaposed to firefly luciferase. The cells were treated with either IL-6, nicotine, T7 HspB4, or Tau 623-628 for 4 h, lysed, and treated with luciferin and ATP, and the resulting chemiluminescence measured on a luminometer (Fig. 3). The induction of luciferase gene expression resulting in the chemiluminescence indicates that in addition to IL-6 and nicotine, which are known to stimulate Stat3, T7 HspB4 and Tau 623-628 also activate this pathway.

Common Pattern of Inhibition of LPS-Induced Proinflammatory Cytokines. Amyloid fibrils, sHsps, and nicotine have been shown to reduce the proinflammatory cytokines IL-6, IL-1β, and TNF-α (2, 6, 8, 9, 24, 31); consequently, further confirmation of this inhibition in

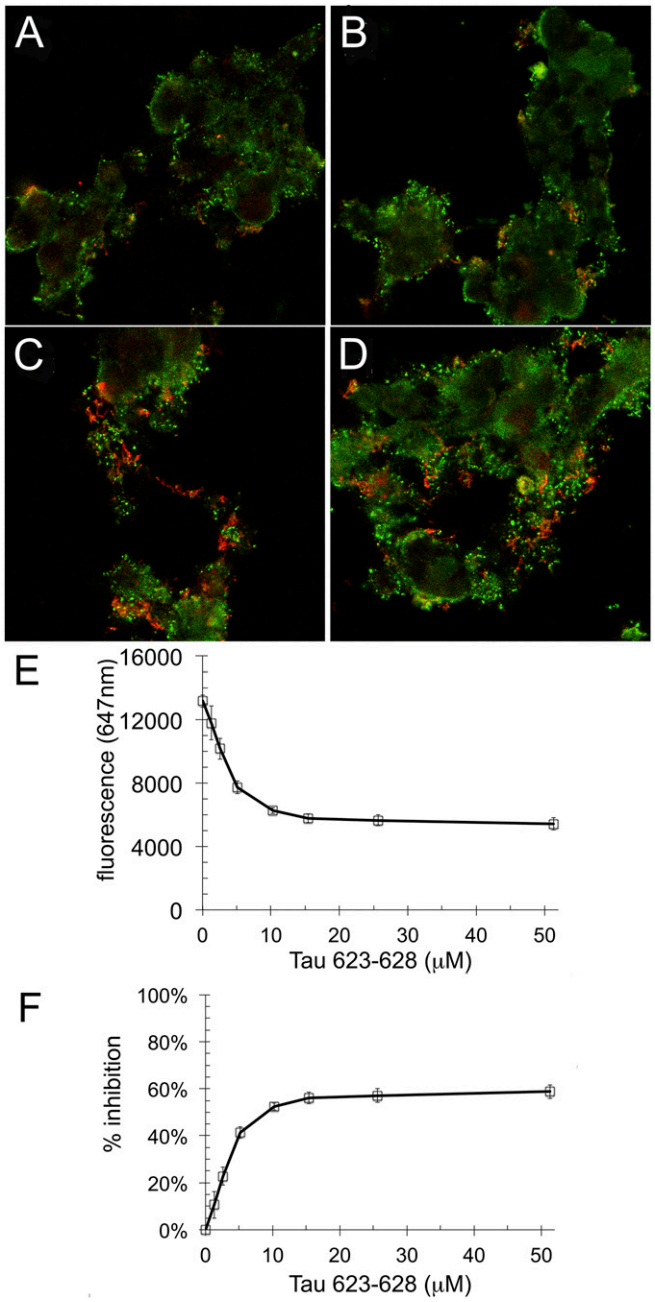

Fig. 2. Whole-cell inhibition assays demonstrate that T7 HspB4 and amyloid fibrils composed of Tau 623-628 inhibit α-bungarotoxin binding. (*A–D*) Micrographs of HEK-293 cells demonstrating that increasing levels of FITC-T7 HspB4 (*A* and *B*: 30 μM; *C* and *D*: 15 μM) reduce binding of Alexa 647-labeled α-bungarotoxin (2.5 μM). Measurement of intensity of fluorescent signal/unit area results in ~50% inhibition (*SI Appendix*, Table S2). (*E* and *F*) Using flow cytometry, incubation of increasing amounts of Tau 623-628 was shown to reduce binding of Alexa 488-labeled α-bungarotoxin on the surface of HEK-293 cells (*E*), and the data were replotted as percent inhibition (*F*).

murine systems was unnecessary. However, in humans, the α7 NAChR gene is partially duplicated and a second receptor, *ChrFam7a*, is differentially expressed (32). The partial duplication results in the deletion of the leader sequence and the first four exons and the fusion with several exons of the unc-51–like kinase 4 gene. The functional role of the modified receptor is controversial, with several reports assigning the protein as a dominant negative based on its inability to flux Ca^{+2} (33, 34).

U937 cells, a human monocytic cell line, exclusively express *ChrFam7a* with no detectable *Chrna7* (*SI Appendix*, Fig. S1). Consequently, stimulating this cell line with LPS to induce IL-6 and treating with the set of NAChR agonists both allows their inhibitory activity to be compared and demonstrates the signaling potential of the mutated human receptor. U937 cells were preincubated with varying concentrations of nicotine, AR-R17779 (α7-specific agonist), Amylin 28-33, T7 HspB4, and Tau 623-628 and stimulated with LPS, and the proinflammatory cytokines in the supernatants 18 h later were measured by ELISA (IL-6, Fig. 4*A*) and using a luminex kit for 52 cytokines (Fig. 4*B*). Nicotine, AR-R17779, T7 HspB4, and amyloid fibrils composed of Tau 623-628 or Amylin 28-33 all inhibited IL-6 production from LPS-stimulated U937 cells, indicating a common pathway, and the compounds were functional agonists of *ChrFam7a*. Measurement of the cytokines in the supernatant of the treated cells revealed a reduction not only in IL-6, IL-1β, and TNF-α, but also in IL-8, IL-18, IL-9, and VEGF. The pattern of inhibition seen in the case of the small molecules nicotine and AR-R17779 mirrored that observed for T7 HspB4 and the fibrils composed of either Tau 623-628 or Amylin 28-33. The only exception was IL-8, which was more effectively inhibited by Tau fibrils and T7 HspB4. Collectively, the data support the premise that each of these compounds is an α7 NAChR agonist signaling through a common immune-suppressive pathway, and the mutated *ChrFam7a* is shown to be a functional receptor.

Induction of Autophagy. In addition to inhibiting proinflammatory gene expression (35), nicotine reduces IL-1β secretion by inducing autophagy and the subsequent metabolism of inflammasomes (17, 36, 37). Autophagy initially was measured using HEK-293 cells transfected with a commercially available insect baculovirus vector containing a mammalian promoter encoding LC3-GFP. As a negative control, cells were transfected with LC3 G/A GFP, in which the C-terminal glycine is mutated to alanine, preventing modification with phosphatidylethanolamine. The cells were stimulated separately with nicotine, AR-R17779, T7 HspB4, and fibrils composed of Tau 623-628. After 6 h, the cells were treated with 0.1% saponin, and the amount of autophagy was observed using confocal microscopy (Fig. 5 *A–D*). In each case, there was clear perinuclear punctate staining, with the exception of cells transfected with LC3 G/A GFP (Fig. 5*E*) and untreated transfected cells (Fig. 5*F*). Alternatively, HEK-293 cells were stimulated with LPS and treated with nicotine, T7 HspB4, and fibrils

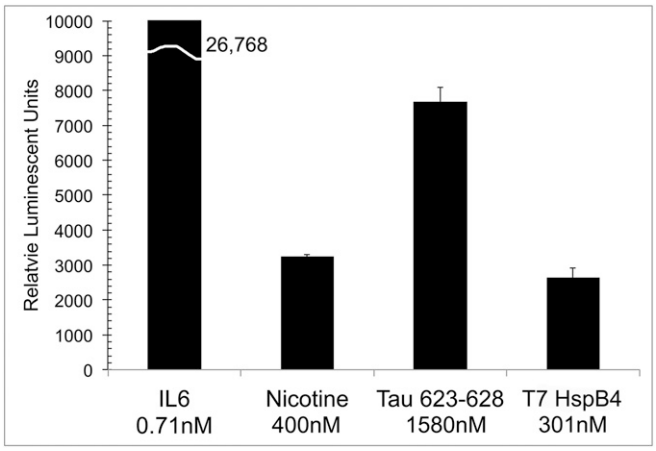

Fig. 3. IL-6, nicotine, T7 HspB4, and amyloid fibrils composed of Tau 623-628 stimulate Stat3 signaling. Graph of relative chemiluminescence produced by HEK-293 cells transfected with a reporter plasmid containing luciferase with an SIE promoter and stimulated with the different agonists. Values in graph represent mean ± SD.

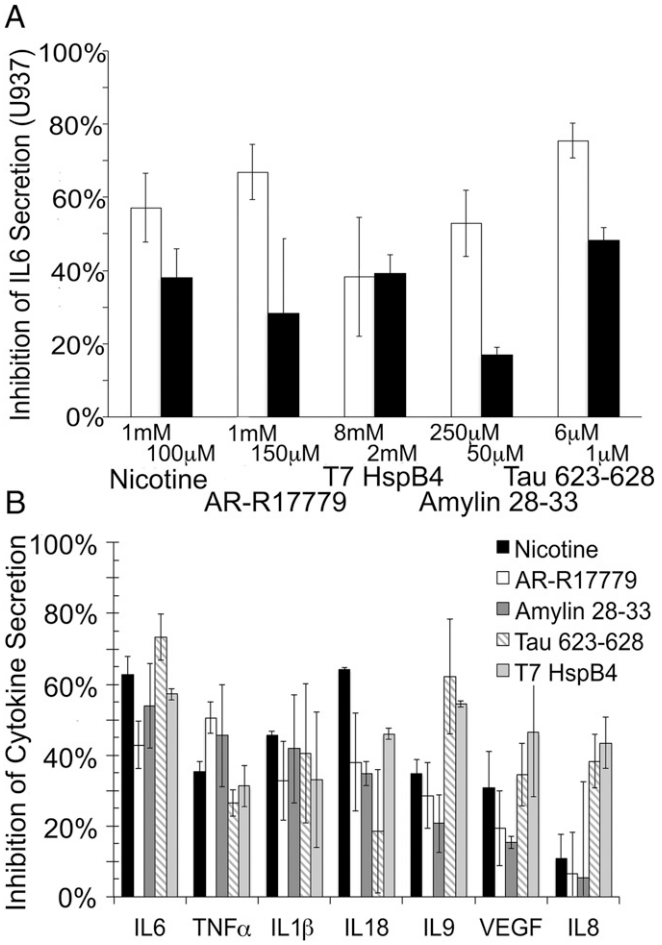

Fig. 4. A similar pattern of inhibition of cytokine secretion when the human monocytic cell line U937 is pretreated with a set of NAChR agonists before stimulation with LPS. (*A*) Percent inhibition of IL-6 secretion after LPS stimulation in the presence of varying concentrations of NAChR agonists, measured by ELISA. (*B*) Percent inhibition of a set of cytokines in the supernatant of U937 cells after LPS stimulation, measured using a Luminex assay. Values in graph represent mean ± SD.

composed of Tau 623-628 for 16 h. The cells were permeabilized with 0.1% saponin and treated with fluorescently labeled anti-LC3. The cells were washed and analyzed by flow cytometry. Using this procedure resulted in a clear distinction between cells stimulated with nicotine, T7 HspB4, and Tau 623-628 compared with untreated cells or those treated with LPS alone (Fig. 5*G*).

Role of α7 NAChR Expression and the Presence of B Lymphocytes in the Therapeutic Effect of NAChR Agonists, Amyloid Fibrils, and sHsps in EAE. Nicotine, AR-R17779, amyloid fibrils, and sHsps all are effective therapeutics for EAE in wild-type animals (6–9, 13–17). The therapeutic effects of nicotine are reduced significantly in α7 NAChR-knockout animals, whereas amyloid fibrils and sHsps have been shown to require presence of B1a cells for efficacy (8). If all these reagents induce a common immune-suppressive pathway based on binding to α7 NAChR, then nicotine and AR-R17779 also should be ineffective in B cell-deficient μMT mice, while the fibrils and sHsps should require the expression of α7 NAChR.

The results of a series of experiments analyzing each of these combinations are shown in Fig. 6. In each case, EAE was induced with murine MOG 35-55, and the animals were treated with daily i.p. injections with the different compounds beginning at the onset of paralytic signs (day 12). Consistent with binding α7 NAChR, treatment with either Amylin 28-33 or T7 HspB4 was effective in wild-type animals, but not in α7 NAChR-knockout mice (Fig. 6 *A*–*D*). AR-R17779 and PNU-120596 (an α7 NAChR-specific positive allosteric modulator) also were therapeutic in wild-type animals (Fig. 6 *E* and *F*) but, along with nicotine, did not modulate the paralytic symptoms in μMT mice (Fig. 6 *G* and *H*), indicating a need for B cell involvement, most likely B1a lymphocytes based on our previous experiments (8).

Discussion

The data in this manuscript support the premise that amyloid fibrils and sHsps are α7 NAChR agonists, binding at or near the orthosteric site and stimulating Stat3 signaling and autophagy. The activation of the receptor leads to the reduction of the proinflammatory cytokines TNF-α, IL-1β, IL-6, and IL-18 and, in EAE, the reduction of paralysis. The studies are consistent with earlier work establishing that amyloid β binds several NAChRs (including α7 NAChR) and signals through Stat3 (10, 11), as well as with prior studies demonstrating that nicotine was therapeutic in EAE (13–16). The clarification of a receptor for the two types of biologics enhances the understanding of their mode of action and allows the present studies to be compared with the extensive

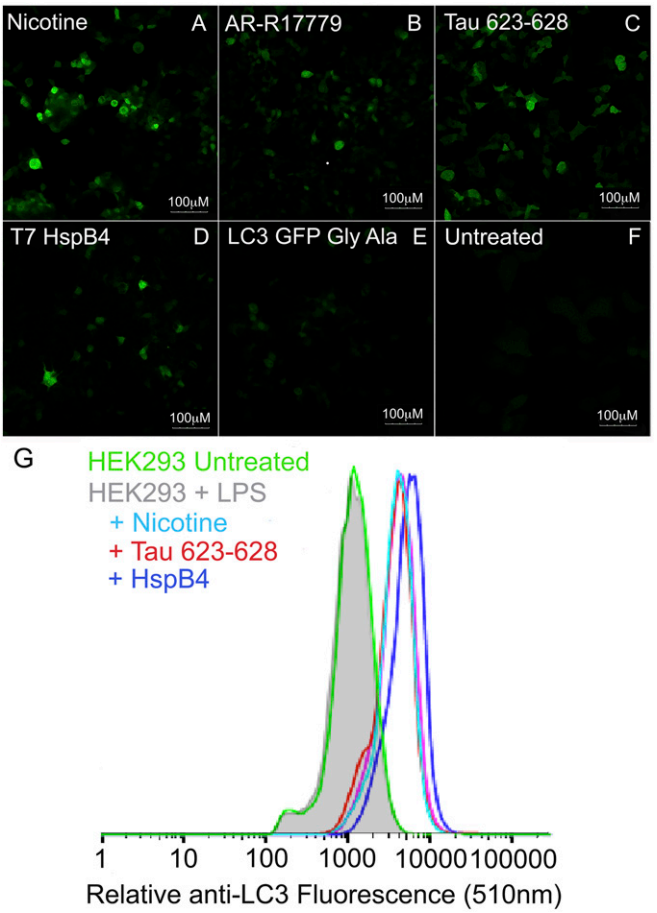

Fig. 5. Induction of autophagy analyzed by microscopy (*A*–*F*) or flow cytometry (*G*). (*A*–*D*) HEK cells transfected with LC3-GFP were treated with (*A*) nicotine (18.8 μM), (*B*) AR-R17779 (65.8 μM), (*C*) Tau 623-628 (1.26 μM), and (*D*) T7 HspB4 (150 nM). (*E*) Cells transfected with LC3 G/A GFP were treated with nicotine (18.8 μM). (*F*) Untreated, transfected cells. (G) For FACS analyses, HEK-293 cells were activated with LPS (100 ng/mL) and treated with each of the agonists for 16 h. The cells were removed from the six-well plates with Ca^{+2}/Mg^{+2}-free PBS, permeabilized with 0.1% saponin, treated with fluorescent anti-LC3 for 30 min, and washed; the resultant fluorescence was measured using flow cytometry.

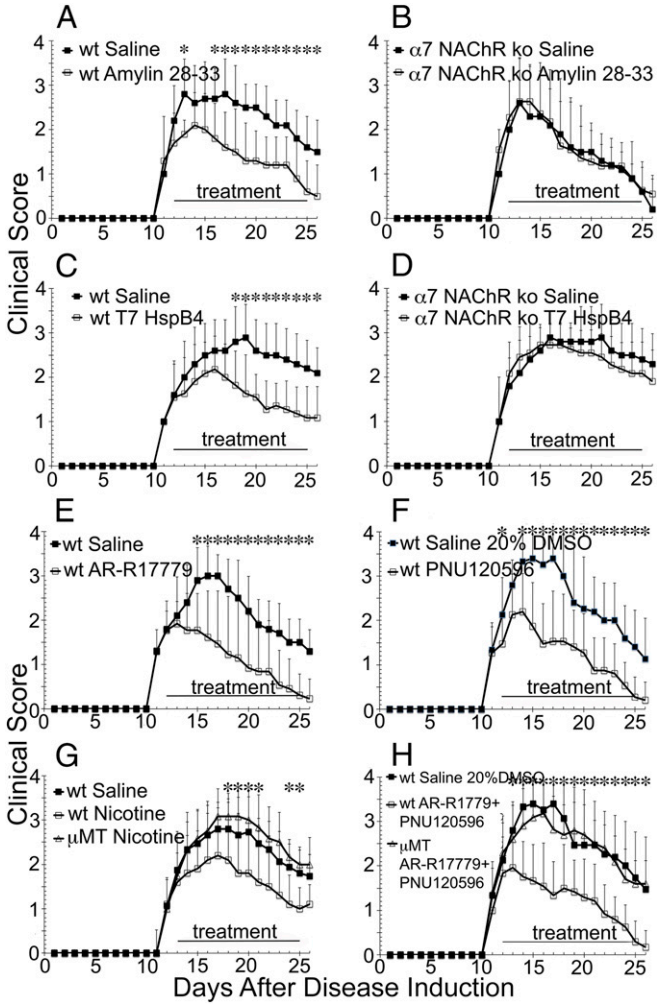

Fig. 6. Differential therapeutic effects in female C57BL/6 wild-type mice compared with α7 NAChR-knockout (ko) animals and C57BL/6 μMT mice when treated with Amylin 28-33, T7 HspB4, AR-R17779, PNU120596, or nicotine. Wild-type and α7 NAChR$^{-/-}$ mice with EAE were treated daily with i.p. injections of 10 μg of Amylin 28-33 (n = 11) (*A* and *B*) or 20 μg of T7 HspB4 (n = 11) (*C* and *D*) at onset of symptoms. Wild-type mice with EAE were treated daily with i.p. injections of 5 mg/kg of AR-R17779 (n = 13) (*E*) or 2.5 mg/kg PNU120596 (n = 15) (*F*). Wild-type and μMT mice were treated daily with 5 mg/kg nicotine (n = 15) (*G*) and a mixture of 0.5 mg/kg AR-R17779 and 2.5 mg/kg PNU120596 (n = 15) (*H*). Values in graph represent mean ± SD; *P < 0.05 calculated by two-tailed Mann–Whitney U test.

publications revealing that binding to α7 NAChR activates a potent antiinflammatory pathway.

These studies complement the novel discoveries by Tracey and coworkers (26), who revealed that the nervous system modulates the immune response via activation α7 NAChR. Tracey and coworkers (26) established that vagal nerve stimulation in the spleen releases norepinephrine, which activates choline acetyltransferase (*CHAT*) in lymphocytes, producing acetylcholine that binds NAChR in MΦs. We show here that injection of either sHsps or amyloid fibrils induces the immune-suppressive pathway by directly binding NAChR, without involvement of *CHAT*. In addition to peritoneal MΦs, B lymphocytes—in particular IL-10–producing B1a cells—also express α7 NAChR and are activated by sHsps and amyloid fibrils.

Activation of the NAChR by nicotine, amyloid fibrils, and T7 HspB4 stimulates autophagy, providing an additional immune-suppressive pathway in which inflammasomes are metabolized, reducing IL-1β expression (17). In microglia and neutrophils, amyloid β binds NALP3, inducing inflammasome activation and IL-1β production (38), which emphasizes the dual activity of amyloid fibrils. The balance between binding NAChR and NALP3 dictates whether amyloid fibrils are either inflammatory or immune suppressive, which explains the complex duality of the role of amyloid fibrils in disease.

The immune-suppressive pathways stimulated by amyloid fibrils binding NAChR might be a central factor in amyloid-linked neurodegeneration. Our laboratory has documented that Ly6C^{hi} MΦs migrate into the brain in animal models of EAE, but not Huntington's disease or in the mutant sod-1 animal model of ALS (39). A possible explanation for the differences could be the presence of amyloid fibrils in the periphery in the latter two cases, which would inhibit the activation of the Ly6C^{hi} MΦs. The inhibition of the migration of the activated MΦs would limit fibril clearance and exacerbate neuronal death and neurodegeneration. Support for this hypothesis is the recent publication by Schwartz and coworkers (40), who successfully treated mice with Alzheimer's disease with anti-PD1. Blocking this pathway is believed to activate CD8 T lymphocytes in cancer models, but this pathway also is central to the activation process in myeloid cells. In the Alzheimer's model, checkpoint inhibition resulted in an IFN-γ–dependent systemic immune response, which is followed by the recruitment of monocyte-derived macrophages to the brain.

The partial duplication of the α7 NAChR gene to create ChrFam7a is an important issue to consider with future therapies. Overlooking the role of ChrFam7a may have been a factor in the failure of the previous clinical trials of NAChR agonists in treating Alzheimer's disease and schizophrenia. The predominant form of the NAChR on human MΦs is ChrFam7a, whose functional capacity to signal has been controversial because of its failure to flux Ca^{+2}. Here, we demonstrate that the NAChR agonists all suppressed proinflammatory cytokine production in U937 human cells, which exclusively express *ChrFam7a*, arguing that it is a functional receptor. Consequently, partial agonists and positive allosteric modulators specific for *ChrFam7a* may systemically modulate this neuroimmune circuit and reduce inflammation in a broad spectrum of diseases.

Methods

The isolation and purification of murine peritoneal cells and the cloning, expression, and purification of T7 human HspB4 were described previously (6, 8).

Cross-Linking of T7 HspB4 and Tau 623-628 Amyloid Fibrils to Surfaces of Peritoneal MΦs and B1a, B2, and T Lymphocytes. CD11b^{+}F4/80^{high} and CD11b^{+}F4/80^{low} MΦs and B1a (CD19^{+}CD5^{+}), B2 (CD19^{+}CD5^{-}), and T (CD19^{-}CD5^{+}) lymphocytes were purified from peritoneal exudates by flow cytometry and incubated overnight in six-well plates with DMEM lacking methionine and leucine and supplemented with photoreactive leucine (5.72 mg/10 mL) and methionine (3.14 mg/10 mL). The cells were washed and transferred back into the six-well plates with the addition of 10 μg of biotinylated Tau 623-628 or 20 μg of biotinylated T7 HspB4, along with protease inhibitors (Halt; Thermo). After 5 min of incubation, the cells were photolysed with 365-nm light for 15 min. The cells were lysed with 500 μL of radioimmunoprecipitation assay (RIPA) buffer with protease inhibitors at 4 °C for 15 min. The mixture was spun, and the supernatant was incubated with 10 μL of Neutravidin (Thermo Fisher) overnight. The resin was removed from the supernatant by centrifugation and repeatedly washed with RIPA buffer. The resin was reduced, alkylated, and trypsinized, and the resultant peptide fragments were separated using a C18 analytical column. A Bruker Advance Source (Auburn) was used for nanoelectrospray mass ionization. Data acquisition and analysis were done as previously reported (7).

Stat3 Signaling. HEK-293 cells (2 × 10^5 cells per well) grown in a six-well plate were transfected with a commercially available reporter plasmid with the SIE promoter juxtaposed to firefly luciferase (Thermo Fisher) and incubated overnight. The cells were treated with IL-6 (0.7 nM), nicotine (400 nM), T7 HspB4 (301 nM), and Tau 623-628 (1,580 nM) for 4 h, lysed, and treated with luciferin and ATP, and the resulting chemiluminescence was measured on a luminometer.

Induction and Measurement of Autophagy. Punctate staining characteristic of the localization of LC3-GFP in the autophagosome membrane was used to identify whether nicotine and the biologic agents induce autophagy. A commercially available autophagy kit from Thermo Fisher Scientific (Premo Autophagy Sensor LC3B-GFP) was used to quantify autophagy in combination with confocal microscopy. HEK-293 cells grown on chamber slides (1.5×10^5 per chamber; Thermo Fisher) were transfected with an insect baculovirus containing a mammalian promoter encoding LC3-GFP or LC3 G/A GFP and incubated overnight. The following day, nicotine (18.8 μM), AR-R17779 (65.8 μM), PNU-120596 (16.0 μM), T7 HspB4 (150 nM), Tau 623-628 (1.26 μM), and Amylin 28-33 (3.3 μM) were added separately to the cells, which were incubated for an additional 4 h, after which they were washed, fixed, and permeabilized with 0.1% saponin to remove the LC3-GFP or LC3-GFP G/A not associated with the autosome membrane. The cells were visualized using a Leica TCS SP8 White Light Laser confocal microscope. For FACS analyses, a different commercial kit was used (Muse Autophagy Kit; MilliporeSigma), in which HEK-293 cells were grown in six-well plates, activated with LPS (100 ng/mL), and treated with each of the agonists for 16 h. The cells were removed from the six-well plates with Ca^{+2}/Mg^{+2}-free PBS, permeabilized with 0.1% saponin, treated with fluorescent anti-LC3 for 30 min, and washed, and the resultant fluorescence was measured using flow cytometry.

Competition Between α-Bungarotoxin and T7 HspB4 or Tau 623-628. HEK-293 cells grown in chamber slides (1.5×10^5 per chamber; Thermo Fisher) were cooled to 4 °C and treated with FITC-T7 HspB4 (15 or 30 μM) for 5 min before the addition of Alexa 647-labeled α-bungarotoxin (2.5 μM). Cells were incubated a further 30 min at 4 °C, washed, fixed (1% paraformaldehyde), and visualized using a Leica TCS SP8 White Light Laser confocal microscope. The relative amounts of red and green were measured per unit area (*SI Appendix*, Table S2). Inhibition of Alexa 488-labeled α-bungarotoxin (2.5 μM) binding with Tau 623-628 (0 to 50 μM) was performed similarly but analyzed by flow cytometry.

Inhibition of IL-6 Secretion in U937 Cells in Vitro After LPS Challenge. U937 cells (10^6/mL) were plated in a 96-well plate and treated with nicotine (1,000 to 1 μM), AR-R17779 (1,000 to 1 μM), Amylin 28-33 (825 μM to 825 nM), T7 HspB4 (50 μM to 50 nM), or Tau 623-628 (50 to 1.5 nM). Thirty minutes later, LPS (*Escherichia coli* endotoxin 0111:B4; Sigma) (100 ng/mL) was added and the samples were incubated for 16 h. BD Biosciences anti-human IL-6 OptEIA kits were used to determine the IL-6 concentrations in triplicate in each treatment group. eBioscience/Affymetrix Magnetic Bead 63-Plex Luminex kits were used according to the manufacturer's recommendations.

Induction of Active EAE in Mice by Immunization with MOG and Adjuvant. EAE was induced in female wild-type C57BL/6 mice or μMT mice on C57BL/6 background (The Jackson Laboratory) by procedures previously described (6). All animal protocols were approved by the Institutional Animal Care and Use Committee at Stanford University.

ACKNOWLEDGMENTS. We thank Chris Adams, Ryan Lieb (mass spectrometry), Bianca Gomez (flow cytometry), and Kitty Lee (microscopy) for their technical assistance. Cell sorting/flow cytometry analysis for this project was done on an instrument in the Stanford Shared FACS Facility obtained using National Institutes of Health S10 Shared Instrument Grant S10RR025518-01. The microscopy was performed on a shared confocal microscope supported, in part, by Award 1S10OD010580 from the National Center for Research Resources. This work was funded by a grant from the National Multiple Sclerosis Society (to L. Steinman). L. Steinman and J.B.R. have a patent application filed via Stanford University covering aspects of the work described herein.

1. Chabas D, et al. (2001) The influence of the proinflammatory cytokine, osteopontin, on autoimmune demyelinating disease. *Science* 294:1731–1735.
2. Ousman SS, et al. (2007) Protective and therapeutic role for alphaB-crystallin in autoimmune demyelination. *Nature* 448:474–479.
3. Arac A, et al. (2011) Systemic augmentation of alphaB-crystallin provides therapeutic benefit twelve hours post-stroke onset via immune modulation. *Proc Natl Acad Sci USA* 108:13287–13292.
4. Velotta JB, et al. (2011) αB-crystallin improves murine cardiac function and attenuates apoptosis in human endothelial cells exposed to ischemia-reperfusion. *Ann Thorac Surg* 91:1907–1913.
5. Pangratz-Fuehrer S, Kaur K, Ousman SS, Steinman L, Liao YJ (2011) Functional rescue of experimental ischemic optic neuropathy with αB-crystallin. *Eye (Lond)* 25:809–817.
6. Kurnellas MP, et al. (2012) Chaperone activity of small heat shock proteins underlies therapeutic efficacy in experimental autoimmune encephalomyelitis. *J Biol Chem* 287: 36423–36434.
7. Kurnellas MP, Adams CM, Sobel RA, Steinman L, Rothbard JB (2013) Amyloid fibrils composed of hexameric peptides attenuate neuroinflammation. *Sci Transl Med* 5: 179ra42.
8. Kurnellas MP, et al. (2015) Amyloid fibrils activate B-1a lymphocytes to ameliorate inflammatory brain disease. *Proc Natl Acad Sci USA* 112:15016–15023.
9. Kurnellas MP, et al. (2014) Mechanisms of action of therapeutic amyloidogenic hexapeptides in amelioration of inflammatory brain disease. *J Exp Med* 211:1847–1856.
10. Wang HY, et al. (2000) Beta-amyloid(1-42) binds to alpha7 nicotinic acetylcholine receptor with high affinity. Implications for Alzheimer's disease pathology. *J Biol Chem* 275:5626–5632.
11. Wang HY, Lee DH, Davis CB, Shank RP (2000) Amyloid peptide Abeta(1-42) binds selectively and with picomolar affinity to alpha7 nicotinic acetylcholine receptors. *J Neurochem* 75:1155–1161.
12. Pavlov VA, Tracey KJ (2017) Neural regulation of immunity: Molecular mechanisms and clinical translation. *Nat Neurosci* 20:156–166.
13. Gao Z, Nissen JC, Ji K, Tsirka SE (2014) The experimental autoimmune encephalomyelitis disease course is modulated by nicotine and other cigarette smoke components. *PLoS One* 9:e107979.
14. Hao J, et al. (2011) Attenuation of CNS inflammatory responses by nicotine involves α7 and non-α7 nicotinic receptors. *Exp Neurol* 227:110–119.
15. Jiang W, et al. (2016) Infiltration of CCR2+Ly6Chigh proinflammatory monocytes and neutrophils into the central nervous system is modulated by nicotinic acetylcholine receptors in a model of multiple sclerosis. *J Immunol* 196:2095–2108.
16. Shi FD, et al. (2009) Nicotinic attenuation of central nervous system inflammation and autoimmunity. *J Immunol* 182:1730–1739.
17. Shao BZ, et al. (2017) Autophagy plays an important role in anti-inflammatory mechanisms stimulated by alpha7 nicotinic acetylcholine receptor. *Front Immunol* 8:553.
18. Dineley KT, Bell KA, Bui D, Sweatt JD (2002) Beta-amyloid peptide activates alpha 7 nicotinic acetylcholine receptors expressed in Xenopus oocytes. *J Biol Chem* 277: 25056–25061.
19. Hascup KN, Hascup ER (2016) Soluble amyloid-β42 stimulates glutamate release through activation of the α7 nicotinic acetylcholine receptor. *J Alzheimers Dis* 53:337–347.
20. Tong M, Arora K, White MM, Nichols RA (2011) Role of key aromatic residues in the ligand-binding domain of alpha7 nicotinic receptors in the agonist action of beta-amyloid. *J Biol Chem* 286:34373–34381.
21. You H, et al. (2012) Aβ neurotoxicity depends on interactions between copper ions, prion protein, and *N*-methyl-D-aspartate receptors. *Proc Natl Acad Sci USA* 109: 1737–1742.
22. López-Menéndez C, et al. (2009) Kidins220/ARMS downregulation by excitotoxic activation of NMDARs reveals its involvement in neuronal survival and death pathways. *J Cell Sci* 122:3554–3565.
23. Hogan-Cann AD, Anderson CM (2016) Physiological roles of non-neuronal NMDA receptors. *Trends Pharmacol Sci* 37:750–767.
24. Filippini P, Cesario A, Fini M, Locatelli F, Rutella S (2012) The Yin and Yang of non-neuronal α7-nicotinic receptors in inflammation and autoimmunity. *Curr Drug Targets* 13:644–655.
25. Kalkman HO, Feuerbach D (2016) Modulatory effects of α7 nAChRs on the immune system and its relevance for CNS disorders. *Cell Mol Life Sci* 73:2511–2530.
26. Olofsson PS, Rosas-Ballina M, Levine YA, Tracey KJ (2012) Rethinking inflammation: Neural circuits in the regulation of immunity. *Immunol Rev* 248:188–204.
27. Olivares D, et al. (2012) N-methyl D-aspartate (NMDA) receptor antagonists and memantine treatment for Alzheimer's disease, vascular dementia and Parkinson's disease. *Curr Alzheimer Res* 9:746–758.
28. Pavlov VA, Tracey KJ (2012) The vagus nerve and the inflammatory reflex–Linking immunity and metabolism. *Nat Rev Endocrinol* 8:743–754.
29. de Jonge WJ, et al. (2005) Stimulation of the vagus nerve attenuates macrophage activation by activating the Jak2-STAT3 signaling pathway. *Nat Immunol* 6:844–851.
30. Lee RH, Vazquez G (2013) Evidence for a prosurvival role of alpha-7 nicotinic acetylcholine receptor in alternatively (M2)-activated macrophages. *Physiol Rep* 1: e00189.
31. Wang TS, Deng JC (2008) Molecular and cellular aspects of sepsis-induced immunosuppression. *J Mol Med (Berl)* 86:495–506.
32. Sinkus ML, et al. (2015) The human CHRNA7 and CHRFAM7A genes: A review of the genetics, regulation, and function. *Neuropharmacology* 96:274–288.
33. Araud T, et al. (2011) The chimeric gene CHRFAM7A, a partial duplication of the CHRNA7 gene, is a dominant negative regulator of α7*nAChR function. *Biochem Pharmacol* 82:904–914.
34. de Lucas-Cerrillo AM, et al. (2011) Function of partially duplicated human α77 nicotinic receptor subunit CHRFAM7A gene: Potential implications for the cholinergic anti-inflammatory response. *J Biol Chem* 286:594–606.
35. Yoshikawa H, et al. (2006) Nicotine inhibits the production of proinflammatory mediators in human monocytes by suppression of I-kappaB phosphorylation and nuclear factor-kappaB transcriptional activity through nicotinic acetylcholine receptor alpha7. *Clin Exp Immunol* 146:116–123.
36. Harris J, et al. (2011) Autophagy controls IL-1beta secretion by targeting pro-IL-1beta for degradation. *J Biol Chem* 286:9587–9597.
37. Samie M, et al. (2018) Selective autophagy of the adaptor TRIF regulates innate inflammatory signaling. *Nat Immunol* 19:246–254.
38. Halle A, et al. (2008) The NALP3 inflammasome is involved in the innate immune response to amyloid-beta. *Nat Immunol* 9:857–865.
39. Ajami B, et al. (2018) Single-cell mass cytometry reveals distinct populations of brain myeloid cells in mouse neuroinflammation and neurodegeneration models. *Nat Neurosci* 21:541–551.
40. Baruch K, et al. (2016) PD-1 immune checkpoint blockade reduces pathology and improves memory in mouse models of Alzheimer's disease. *Nat Med* 22:135–137.